Zirconium dioxide membranes decorated by silanes based-modifiers for membrane distillation – Material chemistry approach

Joanna Kujawa, Wojciech Kujawski, Sophie Cerneaux, Guoqiang Li, Samer Al-Gharabli

Journal of Membrane Science 596 (2020) 117597

Contents lists available at ScienceDirect

Journal of Membrane Science

journal homepage: http://www.elsevier.com/locate/memsci

Zirconium dioxide membranes decorated by silanes based-modifiers for membrane distillation – Material chemistry approach

Joanna Kujawa [a,*], Wojciech Kujawski [a], Sophie Cerneaux [b], Guoqiang Li [a], Samer Al-Gharabli [c,**]

[a] Nicolaus Copernicus University in Toruń, Faculty of Chemistry, 7 Gagarina St, 87-100, Toruń, Poland
[b] Institut Européen des Membranes, IEM - UMR 5635, ENSCM, CNRS, Univ Montpellier, Montpellier, France
[c] Pharmaceutical and Chemical Engineering Department, German-Jordanian University, Amman, 11180, Jordan

ARTICLE INFO

Keywords:
ZrO_2 ceramics
Air-gap membrane distillation
Functionalization
Material physicochemical properties
Desalination

ABSTRACT

Zirconium dioxide membranes (3 nm and 200 nm) were chemically modified by silane-based modifiers with different degrees of fluorination. Comprehensive material characterization has been performed before and after the modification process by goniometric, and microscopic techniques. Wetting properties has been accomplished by applying the Zisman method, Kao diagram, spreading pressure, and critical surface tension. The mechanical, tribological, and separation features of all membranes were investigated as a function of grafting time for 5h, 15h, and 35h.The performance of the membrane was assessed in air-gap membrane distillation processes. Non-fluorinated membranes possessed better transport properties and better mechanical stability in comparison with fluorinated ones which enable the generation of porous, hydrophobic, crack-free material, optimized for MD. Grafting with short fluorocarbon chains (FC6) produced highly hydrophobic materials (CA = 145°) with low roughness (R_q = 6.58 nm) compared to grafting with long fluorocarbon chains (FC12). On the other hand, FC6 showed a highly permeable character and elimination of problems related to substantial flux reduction and pore blocking.

1. Introduction

Membrane distillation (MD) is a thermally driven membrane-based separation process in which the applied separation materials have to be porous, hydrophobic, and non-wettable. During the MD separation, only vapours should pass through the membrane porous structure. This property is related to the fact that volatile components in the liquid phase of the feed, evaporate at the pore entrance. Subsequently, mass transfer through the porous membrane occurs in a vapour phase [1,2]. The rejection of non-volatile components, such dissolved salts, and colloids is close to 100% [1,3]. The driving force in MD is related to the difference in chemical potential generated by the differences in the transmembrane temperature or by a decrease of vapour pressure on the permeate side by a sweeping gas or vacuum [3]. Owing to a number of MD advantages, e.g. application of lower operating temperatures comparing with classical distillation, MD can be used for the treatment of temperature-sensitive feed solutions e.g., in the pharmaceutical and food industries [4].

To prevent heat loss through the membrane, materials with low thermal conductivities are required. In the MD process, several parameters affecting the heat map across the setup including membrane type, thickness, porosity, air-gap, material (type, and thickness) of support, and heat polarization. [5]. Ceramic membranes are usually asymmetric multilayer material consisting of a permselective thin film on one or a series of porous supports that provide the necessary mechanical stability with a minimum transport resistance [6]. During the separation processes, it is essential to consider both the selective layer and support in ceramic membranes. Although the feature of a selective layer is important, the resistance of the substrate is not negligible and sometimes could be the main contributor in total mass transport resistance [7]. Many efforts have been made to acquire high flux during the MD process by optimizing the membrane structure (e.g. distribution of pore size, tortuosity, thickness, pore size, and porosity) [8–11]. Even though polymeric membranes have lower thermal conductivity e.g. PE (0.40

* Corresponding author. Faculty of Chemistry, Nicolaus Copernicus University in Toruń, 7 Gagarina Street, 87-100, Toruń, Poland.
** Corresponding author: Pharmaceutical and Chemical Engineering Department, German-Jordanian University, P.O. Box: 35247, Amman, 11180, Jordan.
E-mail addresses: joanna.kujawa@umk.pl (J. Kujawa), samer.gharabli@gju.edu.jo (S. Al-Gharabli).

https://doi.org/10.1016/j.memsci.2019.117597
Received 29 July 2019; Received in revised form 1 October 2019; Accepted 21 October 2019
Available online 24 October 2019

$Wm^{-1}K^{-1}$), PP (0.17 $Wm^{-1}K^{-1}$), and PVDF (0.25 $Wm^{-1}K^{-1}$) [5,12] ceramic membranes have greater thickness in practice which present an important impact on the heat transfer resistance. ZrO_2 membrane has an advantage over other types of ceramic membranes, where the thermal conductivity is in the range of 1.7-2.8 $Wm^{-1}K^{-1}$, compared to the generally used Al_2O_3 (30 $Wm^{-1}K^{-1}$) or TiO_2 (11.8 $Wm^{-1}K^{-1}$) [13].

One of the most critical barriers to the widespread industrial application of membrane distillation is membrane pore wetting [3,5,14–18]. The principal reasons for wetting are the surpass of the liquid entry pressure (LEP) value and the membrane fouling. The pore size of membranes should be as small as possible to provide high LEP. Nonetheless, the membranes possessing smaller pores are usually a subject of lower permeability [7]. Therefore, an asymmetric structure where thin membrane layer docked on a porous support is considered [19]. Taking into account the complexity of asymmetric structure, the material approach in membrane science is essential to optimize membrane efficiency, to increase flux and membrane span life, and to mitigate fouling.

Development in wetting prevention in membrane distillation has been investigated by the introduction of membrane modification, e.g. by hydrophobization [20,21] as well as by the application of pretreatment steps [15].

Generally, polymeric membrane materials, e.g. polyvinylidene fluoride (PVDF), polypropylene (PP), polytetrafluoroethylene (PTFE) are utilized in the MD process owing to the low cost of preparation and excellent transport properties [16,18]. On the other hand, ceramic membranes owing to their robustness and higher stability are more often applied in MD separation thanks to a much higher chemical and thermal resistance, and long-lasting application in comparison to polymeric ones. However, before usage, ceramic materials (e.g., TiO_2, SiO_2, Al_2O_3 or ZrO_2) that are initially hydrophilic need to be hydrophobized for MD processes [22]. Such modification can be accomplished by chemical grafting and/or physical structuring [23,24]. Interesting and efficient modifiers are those possessing alkylsilanes or perfluoroalkylsilanes groups, e.g. perfluorodecyltrichlorosilane [25], hexadecyltrimethoxysilane [7], 1H,1H,2H,2H-perfluorodecyltriethoxysilane [19], 1H,1H,2H,2H-perfluorooctyltrichlorosilane [26]. Alumina membranes (80 nm and 160 nm) modified with perfluorodecyltrichlorosilane were tested by Subramanian at al [25]. in a desalination process by using direct contact MD (DCMD). Membranes were characterized by superhydrophobic character (150° and 161°), and high transport properties of 7.2 and 8.2 $kg\,m^{-2}\,h^{-1}$ for 80 nm and 160 nm membranes, respectively. Hexadecyltrimethoxysilane, non-fluorinated silane, was used during the grafting of 150 nm alumina membrane tested in the VMD process [7]. The long alkyl chain of the modifier caused the highly hydrophobic character of the membrane surface. The contact angle for water was equal to 161°. The modified membrane was characterized by very high permeate flux of 30 $kg\,m^{-2}\,h^{-1}$ in a desalination process of 30 gL^{-1} NaCl solution [7]. Another interesting example of ceramic membrane modification intended for the desalination process of 4 wt% of NaCl solution has been presented by Li and co-workers [27]. The authors prepared of Si_2N_2O nanowires on silica membranes, which were subsequently tested in sweeping gas MD (SGMD). The membranes possessed a contact angle of ca. 160° and transport features of 11.11 $kg\,m^{-2}\,h^{-1}$ [27]. Siyal et al. [28] described the surface modification of SiO_2 glass fibre membranes by fluorographite coating for the desalination process of concentrated saline water containing humic acid by applying DCMD. Amphiphobic membranes (hydrophobic and oleophobic at the same time) were developed by the employment of functionality to surface of the membrane by the fluorographite and polydimethylsiloxane. Modified membranes were tested in DCMD with a feed solution of 1 M NaCl and organic foulant, i.e. 10 mgL^{-1} humic acid [28]. As an effect of modification, an improvement of flux and salt rejection has been pointed out [28]. Another interesting method resulting in the increase of transport properties through the membranes in MD was the immobilization of nanomaterials on the membrane surface (e.g. functionalized carbon nanotubes, and modified silica) [29,30]. The enhancement of flux was also achieved by improving the driving force by photothermal effect [31] or advising Joule heating [32] on a hydrophobic membrane to increase the localized temperature of the membrane surface from the feed side, and subsequently to minimalize the temperature polarization effect. Among the mentioned ceramic materials, zirconia is very interesting materials owing to its high biocompatibility, and outstanding stability [11,33]. On the other hand, zirconia is the least explored ceramic material as a support for ceramic-based membrane separation processes e.g. desalination. So far, the research carried out in the preparation of highly efficient ceramic membranes for desalination process is limited mainly to titania and alumina [8,28]. The application of ZrO_2 membranes was much less explored by the researchers. Krajewski et al. used 200 nm tubular zirconia ceramic membranes in a desalination process of 0.1 gL^{-1} NaCl solution implementing AGMD [34]. Membranes were characterized by flux of ca. 6 $kg\,m^{-2}h^{-1}$ and a very high rejection coefficient of NaCl ~99%. Furthermore, an interesting work has been done by Liu and co-workers [35]. The authors prepared double layer ZrO_2 membranes on a YSZ (yttria-stabilized zirconia) support. The membranes were tested in a DCMD process of 2 wt% NaCl and were characterized by high permeate flux equal to 28.7 $kg\,m^{-2}h^{-1}$.

This study adopted already developed highly capable methods, for the ceramic material hydrophobization, to modify zirconia based-membranes [20,21,36–38]. The main aim of the work was to functionalize ZrO_2 membranes with various modifiers and assess their efficiency in the MD process implemented for desalination by air-gap membrane distillation. Membranes were furnished with alkyl chains possessing varying degrees of fluorination. Additionally, a fluorine-free modifier was also used for comparison. Finally, the separation efficiency of the desalination process was assigned. The physicochemical properties of the novel materials were extensively characterized.

2. Experimental part

2.1. Materials and chemicals

ZrO_2 ceramic membranes ("inside CéRam" series) 5kD and 300kD with flat-sheet and cylindrical geometry were purchased from TAMI (Nyons, France). 1H,1H,2H,2H-perfluorooctyltriethoxysilane (CAS 51851-37-7) marked as FC6; 1H,1H,2H,2H-perfluorodecyltriethoxysilane (CAS 101947-16-4) marked as FC8; and 1H,1H,2H,2H-perfluorotetradecyltriethoxysilane (CAS 885275-56-9) marked as FC12 were bought from SynquestLab (Alachua, USA). n-octyltriethoxysilane (CAS 2943-75-1) labeled as C6 was purchased from Abcr Chemicals (Karlsruhe, Germany). Acetone, butanol, butyl acetate, chloroform (stabilized by 1% ethanol), dimethyl sulfoxide, ethanol, ethyl iodide, methyl *tert*-butyl ether, glycerine, n-hexane, perfluorohexane, pyridine, and sodium chloride were purchased from Avantor Performance Materials Poland S. A (Gliwice, Poland). All the chemicals were applied without additional purification. RO deionized water (18 MΩ cm) was utilized for the NaCl feed solutions preparation.

2.2. Methodology

2.2.1. Membrane grafting process

Chloroform based solutions of grafting agents (0.05 M) were prepared in the ambient atmosphere of argon to avoid polycondensation reaction. Before modification, the membranes were washed successively in acetone, ethanol, and distilled water for 10 min in each solvent and subsequently dried in an oven at 90 °C for 12 h [20,39]. Afterwards, ceramic supports were grafted by soaking samples in the grafting solution for a given period of time (3-steps of modification).

Time of modification steps was as follows 1st step – 5h; 2nd step - 10h, and 3rd step – 20h. After each modification step the membranes were characterized. The efficiency of modification was evaluated for the generated 12 membrane types by measuring the contact angle (for flat-sheet membranes) and water liquid entry pressure (LEPw) (cylindrical

membranes). The hydrophobization process of zirconia ceramics was accomplished accordance with the literature [20,36,38,39]. Transport and separation properties of all membranes were determined in air gap membrane distillation process.

2.2.2. Material characterization of ceramics

The membranes were characterized prior to and after modification by a goniometric technique (Goniometer Attention Theta from Biolin Scientific, Gothenburg, Sweden) employing the tilting plate method in order to determine the apparent contact angle (CA) and sliding angle (SA). 5 s of equilibration time at room temperature were used [38,40]. The presented values are the mean values out of 20–30 separate analyses. The Zisman method [41] was implemented to establish wettability limits given by the critical surface tension of the material (σ_{cr}). The Kao diagram was used to correlate physiochemical features expressed by the roughness parameter (R_q) determined from atomic force microscopy (Atomic force microscopy NanoScope MultiMode SPM System and NanoScope IIIa and Quadrex controller from Veeco, Digital Instrument, Cambridge, UK) with the ability of ceramics to wetting. R_q was determined to base the tip scanning mode for the sample's area of 5 μm × 5 μm. Roughness parameters were calculated by using NanoScope Analysis Software (1.40, Build R3Sr5.96909, 2013 Bruker Corporation). Tribological [20] characterization was done using the following factors determination, Young modulus (E), nanohardness (H_n), and adhesive forces (F_a). The presented values of mentioned parameters were average from 20 measurements in the contact mode (5 times 4 places on the sample) in the case of H and E, and average from 30 measurements for F_a. Wetting was additionally studied by spreading pressure (S) parameter. BET (Brunauer–Emmett–Teller) [42–44] and BJH (Barrett-Joyner-Halenda) [42–44] models were assessed to estimate pore size distribution and pore size of the ceramics basing on the adsorption/desorption isotherms (ASAP 20120 from Micromeritics Instrument Corp., Norcross, USA). Before the isotherm registration, samples were degassed during 2h at 90 °C.

2.2.3. Air-gap membrane distillation

The membrane performance was assessed in the Air-Gap Membrane Distillation process. The experimental protocol and setup were presented in detail elsewhere [21]. The accomplished research possessed the character of fundamental work and for this reason a high driving force was selected, i.e. tests were done at temperatures of 5 °C and 90 °C for permeate and feed solution, accordingly. The subsequent concentrations for feed of NaCl aqueous solutions used were 0 (pure water), 0.25, 0.5, and 1.0 M.

Each membrane sample, after the first, second and third grafting stage was tested in contact with all the feed solutions. The feed was transported along the membranes with the flow rate of 17 L min^{-1}. The time of each experiment varied between 5 and 6h. The first hour was considered as a stabilization step and was not taken into account for the flux calculation. The collected permeate was analysed gravimetrically every 10–15 min. After the AGMD experiment the membrane was washed with DI water and dried overnight in the oven at 60 °C.

The rejection coefficient (R_{NaCl}) of sodium chloride was calculated according to Eq. (1). Dionex DX-100 Ion Chromatograph from Thermo Scientific™ (Dardilly, France) was applied for the evaluation of sodium chloride concentration rejection.

$$R_{NaCl} = \left(1 - \frac{C_p}{C_f}\right) \cdot 100\% \quad (1)$$

where: C_p and C_f stand for the NaCl concentration in permeate and feed solution, respectively.

2.2.4. Wettability study

2.3.2.1. Liquid entry pressure. The principal metric for evaluating membrane wettability is the value of liquid entry pressure (LEP) which was determined for all cylindrical membranes. LEP is the value of the pressure that must be applied to transport liquid (i.e., water) through dry membrane pores [3]. Because LEP depends on the hydrophobicity, surface free energy, liquid surface tension, and maximum pore size of the membrane, consequently, it will depend on the solution composition, operating temperature, surface porosity, surface roughness, and pore shape. Most of the mentioned parameters are related to the modification process which influences surface porosity, surface roughness, and pore shape. LEP must be determined in a precise way. In this work, experimental results were discussed according to Purcell model [45] (Eq. (2)) and its modification proposed by Servi et al. [1].

$$LEP = \frac{-2\gamma_L \cdot \cos(\theta + \alpha)}{r\left(1 + \frac{R}{r}(1 - \cos(\theta + \alpha))\right)} \quad (2)$$

$$sin(\theta + \alpha) = \frac{sin(\theta + \alpha)}{1 + \frac{r}{R}} \quad (3)$$

where R is the fibre/ceramic wall radius and α (Eq. (3)) is the angle under the horizontal at which the liquid meniscus pins prior to advance [3].

The advantage of the Purcell model compared to the Young-Laplace one is the prediction of the positive value of LEP irrespective of CA value. However, this statement can be also inconsistent, because of the fact that many types of membranes can be wetted at a very low value of contact angle. To overcome the mentioned problem, Servi [1] presented approach for all CA values taking into account interactions between pores and testing liquid below the primarily wetted surface by including a "floor" below each pore to the LEP model (Eq. (4)). The mentioned floor defines those fibres/ceramic walls which may permit the liquid to enter further into the membrane. Consequently, LEP can be defined as the pressure at which the liquid splits up from the pore or intercepts the floor, whichever occurs at the lower value of pressure.

$$\frac{r + R(1 - \cos(\alpha))}{-\cos(\theta + \alpha)}(1 - \sin(\theta + \alpha)) = R(1 - \sin(\alpha)) + h \quad (4)$$

where h is the height of "floor" in nm presenting fibres/walls which can attract the liquid to go into the membrane. Authors showed the validation of the model in the range of contact angle between 63° and 129°. Values of r, R and h were determined from scanning electron microscope images.

2.3.2.2. Spreading pressure. Spreading pressure (S) is another parameter utilized for wetting behaviour, expressing the estimation of the tendency of the liquid phase to spread on and/or into the solid phase [46]. Spreading pressure can be defined as a change of work of adhesion (W_{LS}) and work of cohesion (W_s) (Eq. (5)). Correspondingly, it can be presented as a surface tensions difference, separately liquid (σ_L) and solid (σ_S) with interfacial tension (σ_{LS}) (Eq. (6)). The value of S parameter can be either positive or negative. For negative value, the observed wetting is incomplete.

$$S = W_{LS} - W_S \quad (5)$$

$$S = \sigma_L - \sigma_S - \sigma_{LS} \quad (6)$$

2.3.2.3. Zisman plot - critical surface tension. The method is used for the evaluation of wettability behaviour of a solid according to determined critical surface tension (σ_{cr}) applying the contact angles of various liquids. On the Zisman plot [41] the cosine of the contact angle is plotted against the surface tension of the applicable liquid (Fig. S1). Then, the value of the surface tension extrapolated to the cosine of contact angle equal to 1 (for CA = 0°) is referred to as the critical surface tension σ_{cr}. Furthermore, the value of σ_{cr} is taken to the mean value of the surface

free energy of the solid. The determined σ_{cr} values have a crucial practical meaning in the selection of the solvents for membrane cleaning.

2.3.2.4. Kao diagram. Kao diagram is a mighty tool in material science and takes into account the chemical and geometrical factors influencing the hydrophobicity level of the material. By implementing the concept of the Kao diagram [47], it is possible to deliberate the physicochemical features of treated materials regarding wetting abilities and surface roughness. The relation is shown graphically by plotting the cosine of contact angle determined on the rough - θr (real surface) against the Young contact angle determined on a hypothetical smooth flat surface (θ_s). The data are gained from liquids with differentiated value of surface tensions. Highly hydrophilic and less hydrophilic materials are situated in the first part of the coordinate system. For such surfaces, wetting/-soaking of polar solvents to the structure of the material can be noted. In the central part of the Kao diagram, surfaces classified as Wenzel ones are located, having distinguishable homogeneous morphology and hydrophobic character [48]. Finally, highly rough and hydrophobic materials are placed in the Cassie-Baxter zone. That type of surfaces has a well-defined and developed micro- or nano-structure architecture [14].

3. Results and discussion

3.1. The capability of a ceramic material to functionalization

Pristine and modified membranes were extensively studied paying attention to the material features as well as the wetting properties. To evaluate material properties, i.e., ability to grafting, adsorption-desorption nitrogen isotherms were registered before and after modification. The level of interaction among adsorbate and adsorbent could be evaluated by determining the C parameter (Eq. (7)).

$$\frac{1}{\upsilon[(P_0/P)-1]} = \frac{c-1}{\upsilon_m C}\left(\frac{P}{P_0}\right) + \frac{1}{\upsilon_m C} \quad (7)$$

where C is BET constant, P is equilibrium pressure, P_0 is saturation pressure, and υ_m monolayer adsorbed gas quantity.

C constant depends on the quantity of uncovered surface by adsorbate when sufficient adsorption took place in the monolayer and its change is related to the substrate used. For this reason, the chemistry of the surface has significant impact on the C value [49]. Furthermore, the value of C depends on the following variables: pore size, surface porosity, and capacity of adsorption [42,44]. The obtained values of C parameters for ZrO_2 samples were in the range of 58.35 and 8.25. The values for non-modified samples were considered as fairly high. The low values of C exemplify weak gas adsorption related to the low surface area of the material [49].

The observed reduction in C value in respect to pristine samples is a consequence the modification of ceramic materials and the reduction of surface areas. According to the data shown in Fig. 1, it can be seen that the pore size of the original material influences the C value. 5kD unmodified membrane was characterized by a C constant of 22.63, whereas C was equal to 58.35 for a 300kD material. The higher value of C for 300kD can be linked to the higher ability to adsorption, more open structure (pore size equal to ca. 200 nm) and a higher level of available hydroxyl groups on the untreated sample. The higher specific surface would allow anchoring molecules easily into the membrane pore walls. On the other hand, the pore size of the 5kD sample (~3.5 nm) is comparable to the dimension of grafting molecules (1.5–2.3 nm) which generates difficulties for molecules to anchor deeply inside the porous structure (Fig. 1A). The presented data of pore size are overall values for the entire ceramic sample. It needs to be highlighted that ceramic membranes possess a multilayer structure (Figs. S2 and S3) The slightly higher values of C observed for materials treated with non-fluorinated molecules can be explained by a different hydrophobicity level compared with fluorinated analogues analogues (Fig. 1A and B). The different behaviour of modifiers inside the porous structure e.g. by changing pore tortuosity can be observed. Furthermore, a significant decrease in C constant can be caused by divergent interactions with the surface of the ceramic depending on the hydrophobicity, i.e. increasing hydrophobicity with the length of the fluoro-carbon chain. The mentioned effect was visible especially for 300kD-modified membranes (Fig. 1). The value of C factor changed in the range of 19.63–15.86 and 28.08–8.25 for modified 5kD and 300kD ceramics, respectively. To characterize material in a more detailed way, the t-plot method was implemented and used for micropores presence confirmation [42,44]. The thickness of the adsorbed organic nanolayer was calculated according to the Harkins-Jura model and master isotherm relation introduced by Lecloux–Pirrad [44,50,51]. The correlation between the adsorbed layer and relative pressure for chosen ceramics is shown in Fig. 2. For 5kD practically no difference was seen between evaluated samples, irrespective of surface physicochemical features (Fig. 2A). The observed lack of distinction in the thicknesses for 5kD is related to a quite close porous structure, i.e., low porosity ~30% and small pore size ca. 3.5 nm [52]. These observations were supported by pore size changes (Fig. 1A) that were very small for all 5kD membranes. An interesting fact was that the correlation between pore size and length of grafted molecules was not linear. It might be related to the generation of the agglomerated or bundle form of the fluoroalkyl chains. On the other hand, for 300kD ceramics, the reduction of thickness has been observed (Fig. 1B). The thickness of the grafted layer was also examined by TEM

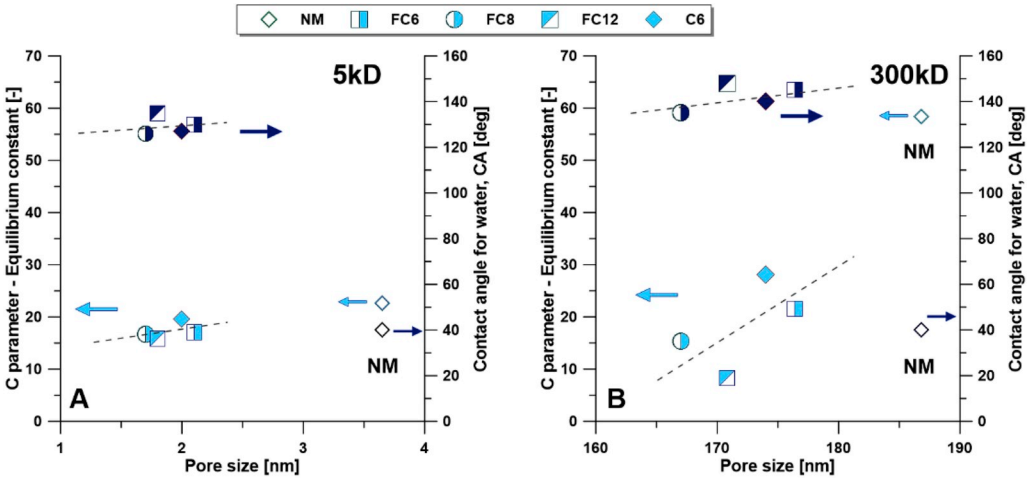

Fig. 1. Correlation between C parameter, contact angle and pore size for pristine and modified ceramics 5kD (A).

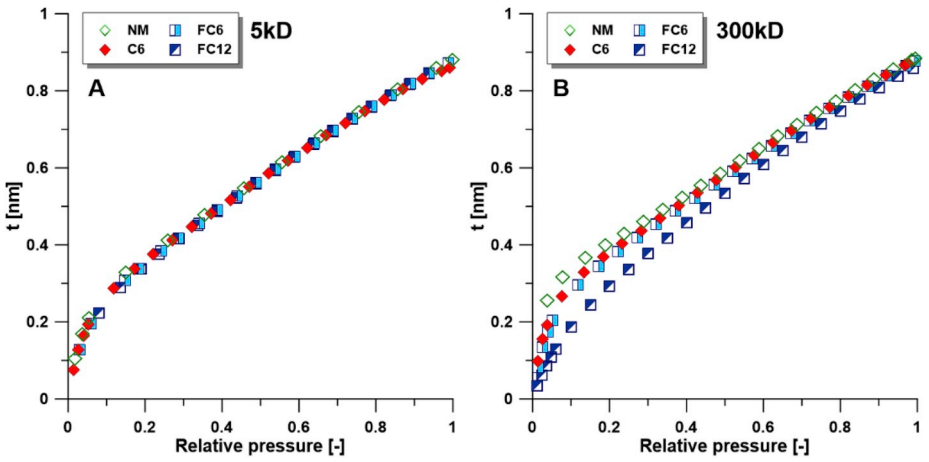

Fig. 2. T-plot – the capability to adsorption on 5kD (A) and 300kD (B) ceramics, pristine and modified membranes.

and EDX. The value of the thickness of organic nanolayer was comparable for both techniques (Figs. S5 and S6). It was correlated to the quite important difference in the pore size as an effect of grafting process (Figs. 1 and S4). It was found that with a growth in the length of fluoro-carbon chain and subsequently with an increase in the hydrophobic character, the reduction of t was seen. It suits well the discussed previously decrease of pore size and membrane tortuosity. Interestingly, the presence or lack of fluorine in the grafting agent has no impact on the adsorbed layer thickness (Fig. 2B).

3.2. *Adjustment of wettability feature by controlling functionalization process*

Since perfluoroalkylsilanes and alkylsilanes are strong surface modifiers, a significant part of the work was dedicated to wettability and studies of the surface. Expectedly, it was observed that the introduction of alkylsilanes and perfluoroalkylsilanes based modifiers on the ceramic ZrO_2 material considerably changed the water contact angle (Fig. 1B). In all cases, a significant increase in CA, from 40° for pristine material up to more than 105° (after 5h of grafting) and >130° (after 35h), has been noted indicating that the modified surface shows a strong hydrophobic character.

To evaluate if the modifiers were covalently attached to the surface, modified membranes were immersed in hexane and were additionally treated by sonication. As shown in Table S1, the CA maintained after both tests, i.e., membranes preserved their hydrophobic character.

The variations of CA for water were related to the role of C-F bonding with the substantial importance meaning of fluorine atoms as well as to the role of C-H bonds [20,53]. In the case of fluorine atoms, their size is much bigger than that of hydrogen atoms. This fact is associated with bigger van der Waals radius (1.47 Å for F and 1.20 Å for H) as well as a cross-section (30 $Å^2$ for F and 20 $Å^2$ for H) [10,53]. The observed differences in CA are related on the one hand to the type of the molecules (length of carbon tail and the presence or lack of fluorine atoms in the molecules) and on the other, to the experimental protocol, i.e. time of modification [20,21]. Depending on the modifiers used, and their orientation on the ceramic surface [54], different values of CA were observed. The trifluoromethyl group in fluorinated compounds (FC6, FC8, and FC12) will give intensification to a strong dipole attributable to modifications in the electronegativity of atoms in a C-F bond that is subsequently revealed by changes of wettability of the functionalized surfaces (Fig. 3). The determined values of CA on the modified materials were in the range of 110 ± 1.5°–148 ± 0.8°. The substantial increase in contact angle was a consequence of the grafting time prolongation from 5h to 35h (Fig. 3). Taking into account the type of modifier, the interesting data were noted for non-fluorinated analogue (C6). Surprisingly,

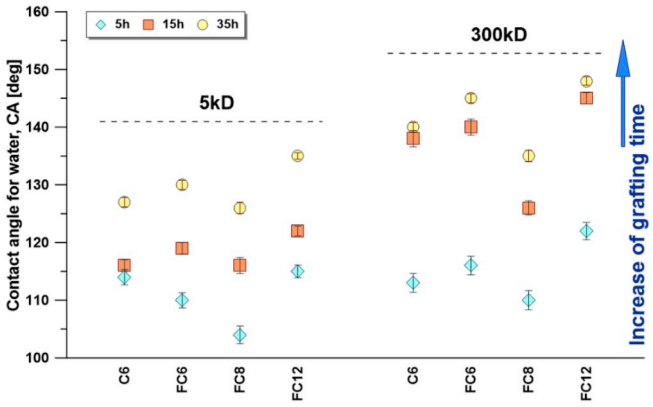

Fig. 3. Evolution of water contact angle after functionalization with various alkylsilanes.

the results were comparable to those achieved for fluorinated agents. A big difference in hydrophobicity has been noted between FC6 and FC12, independently on the pore size of the ceramic (Fig. 3). In that case, the noted variations can be attributed to variations in assembly and structure of both types of grafting agents. Shorter molecules, e.g. C6 and FC6, FC8 can generate vertically oriented structures that are related to the length of the molecules and subsequently with their stronger interaction between grafting molecules and surface. This conclusion is supported by the AFM data (Figs. 4 and 5). Ceramics functionalized with molecules possessing a shorter chain, particularly FC6 and FC8 present an agglomerated structure on the surface causing an increase in the roughness parameter. Such behaviour can also be explained by the potential higher capability of vertical polymerization. An increase in roughness and the thickness of the chemically attached nanolayer is likely to form highly disordered silane clusters [55] (Fig. 5).

As a consequence of the mentioned feature, a reduction in packing density is observed [56]. The most visible rise of the R_q parameter was noted with the prolongation of grafting time (Fig. 4). The revealed alteration was not observed for a surface treated with longer chains, i.e., FC12 (Figs. 2–4). In the case of this latter modifier, the horizontal polymerization is also more favourable [10,53]. The indication of such preferences is observed by the reduced roughness parameter (Fig. 4). According to the literature data, the van der Waals component of the driving force for self-assembly rises with the length of the carbon chain in the modifying molecules [56]. Subsequently, modifiers possessing a longer chain can generate a well-developed molecular organization and therefore less rough material. Alternatively, the hindrance steric effect

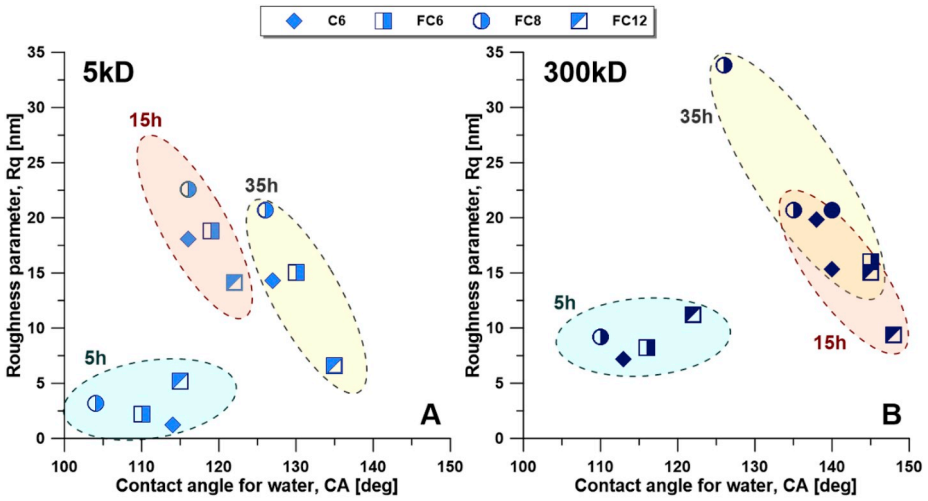

Fig. 4. Correlation of the roughness parameter (R_q) with the contact angle for water, for (A) 5kD and (B) 300kD zirconia membranes modified during 5, 15 and 35h.

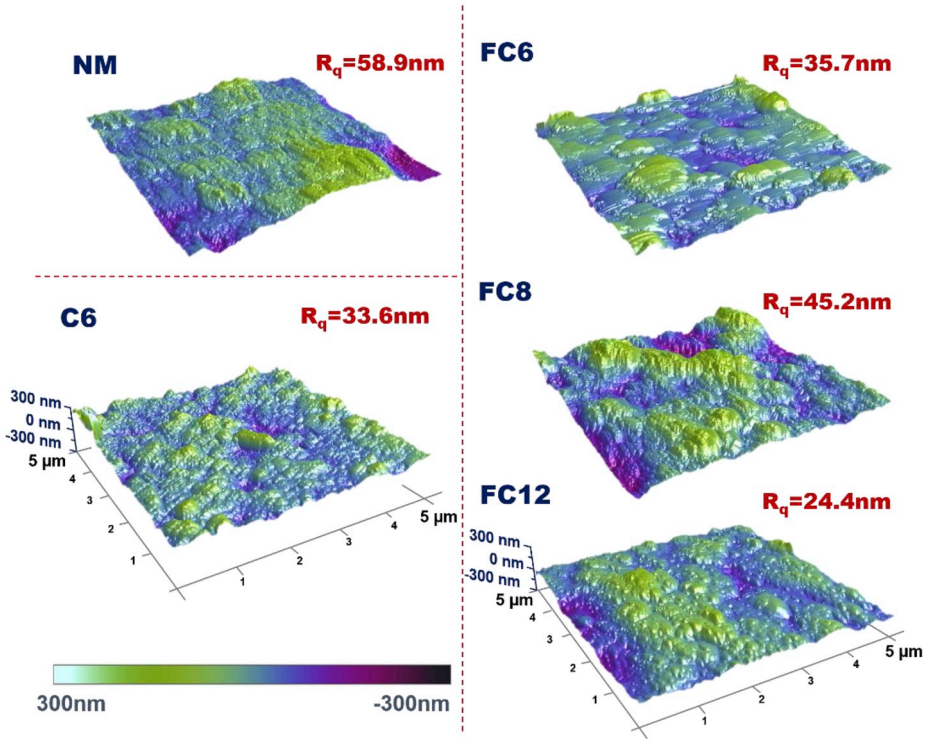

Fig. 5. AFM 3D-profiles for pristine and modified during 5h ZrO_2 300kD membrane.

in the case of longer chains may limit the horizontal crosslinking and condensed packing of grafting molecules during functionalization. Thus, in all cases, defect-free organic nano-layers on the ceramic and inside their porous structure employing repulsive forces to water molecules and preventing in the same time its penetration/soaking in the material were generated.

An interesting correlation has been found between the water contact angle and roughness of the surface (Fig. 4). The reduction of the R_q parameter is observed once more hydrophobic material is created. This observation is in good accordance with other literature findings [10,17,38,53,55,56] and the correlation described above. Furthermore, it was presented that the relation between roughness and hydrophobicity can be adjusted by selecting appropriate grafting agent (with fluorine or fluorine-free, having a certain length of hydrophobic tail) or by duration of modification. Moreover, practically no influence of the ceramic support morphology (i.e., pore size) was noted (Fig. 4). It was stated that C6, FC6, FC12 molecules are the most suitable for the tunable surface properties, generating smooth, and defect-free highly hydrophobic material.

As a result of the wetting measurements, it was found that chosen factors used for wettability assessment changed significantly after modification with alkylsilanes and fluoro-alkylsilanes (Fig. 6). The sliding angle of the surface (Fig. 8A) was reduced after the extension of grafting time from 5h to 35h (5h $SA_{5kD\text{-}C6} = 66 \pm 1.3°$ and 35h $SA_{5kD\text{-}C6} = 41 \pm 1.3°$). The biggest improvement with SA has been found for 300kD-C6 and 300kD-FC6 after increasing the grafting time up to 35h (5h $SA_{300kD\text{-}C6} = 81 \pm 1.6°$ and 35h $SA_{300kD\text{-}C6} = 40 \pm 1.2°$). Comparable values were observed for C6 and FC6 molecules, irrespective of the surface pore size (5kD or 300kD). The highest value was observed for surfaces treated with FC8. This trend is related to the higher roughness

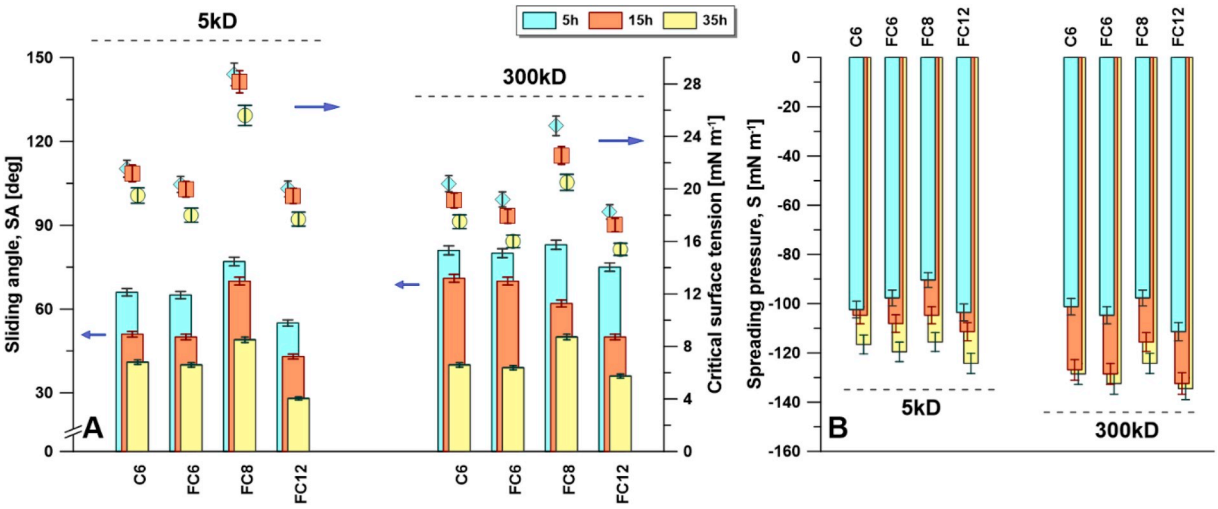

Fig. 6. Wettability features: A – Sliding angle (bars), critical surface tension (points) and B – spreading the pressure of modified ceramics.

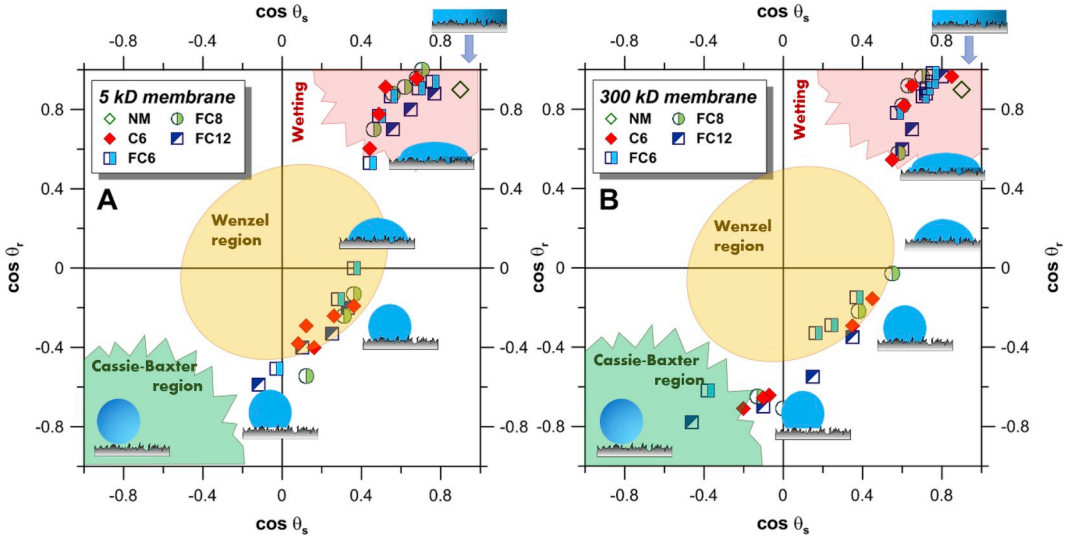

Fig. 7. Kao diagrams for 5kD (A) and 300kD (B) ceramic membranes modified 5h.

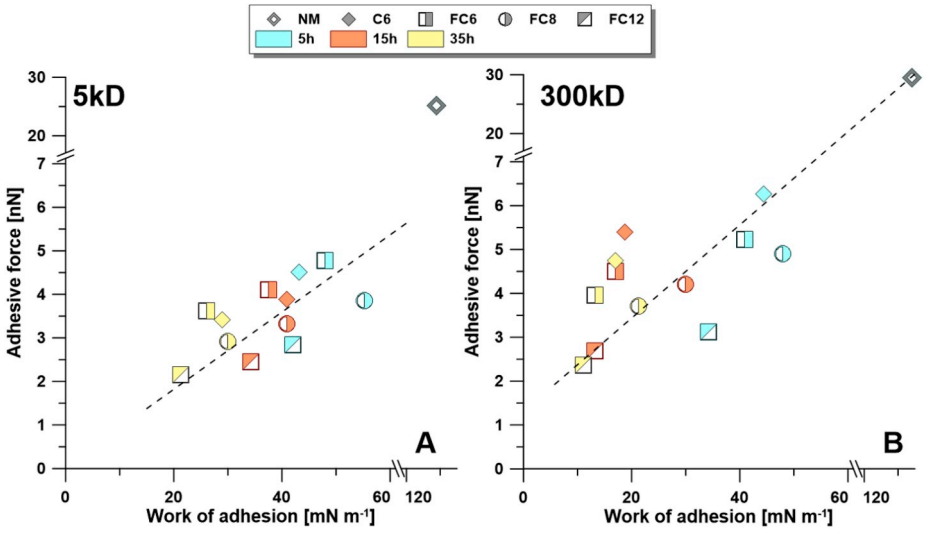

Fig. 8. Adhesive features of the ceramics (A-5kD, B-300kD) and adhesive force in the function of the work of adhesion.

on these ceramics (Fig. 4) and slightly lower hydrophobicity level (Fig. 3). Taking into account the possible application of the ceramics, particularly MD separation, the most important is water resistance to the material during the separation process. To evaluate this property, the critical surface tension (σ_{cr}) and spreading pressure (S) are discussed as the most suitable parameters (described in details in section 2.3.4). When comparing the pristine and modified surface, an important development in critical surface tension was noted (Fig. 6A). Pristine ZrO_2 samples were characterized by 35.5 mN m^{-1} and 30.6 mN m^{-1}, for 5kD and 300kD, respectively. As an effect of the grafting process, these values were reduced to 17.4 ± 0.5 mN m^{-1} (for 5kD) and 15.4 ± 0.4 mN m^{-1} (for 300kD). The mentioned lowest values (reduction of ca. 50%) were achieved for the ceramics modified with FC12 molecules. However, in the presented work, water and NaCl solutions were utilized as feed solutions. The lowest value of liquid tension σ_L for applied feed solution (1 M NaCl) at the temperature of AGMD experiment was 64 mN m^{-1}. For this reason, there is no risk of wetting the grafted membranes during the desalination process. Additionally, it can be mentioned that modification conditions did not substantially influence the critical surface tension value (Fig. 6A). Variations of σ_{cr} for samples treated during 5h and 15h were found to be in the range of the standard deviation.

The spreading pressure was another important parameter, giving a deeper insight into the wetting phenomenon of the modified ceramic membranes. All the determined values were negative (Fig. 6B) being in the range of -134.54 ± 4.4 mN m^{-1} (300kD-FC12 35h grafting) and -89.17 ± 2.9 mN m^{-1} (5kD-FC8 5h grafting). Furthermore, for all samples, CA was higher than zero. These data are in good agreement with the literature findings [57]. S parameters for the pristine sample were equal to -16.71 ± 0.50 mN m^{-1} for 5kD and -11.52 ± 0.34 mN m^{-1} for 300kD, accordingly. The reached negative values of S supported the above-presented data for the incomplete wetting or lack of wetting. Partial wetting was noted only for pristine, non-modified ceramics (Fig. 3). The level of the hydrophobicity of the material influences spreading pressure and wettability feature [57]. Samples with lower hydrophobicity (e.g., 5kD-FC8) are characterized by a smaller S owing to the lower basicity of the material. The generated ceramics were free of wetting and are appropriate for MD application, taking into account all the investigated parameters related to the wettability.

3.3. Influence of the modification process on physicochemistry of ceramic material

In the preparation of new materials, dedicated to membrane distillation, it is essential to assess their stability and water repellency. To achieve the mentioned goals and correlate physicochemical features with wettability changes after the modification process, the Kao diagram can be employed. During the construction of the Kao diagram Wenzel's and Cassie–Baxter's approaches were taken into account (Fig. 7). In Fig. 7, the Kao plot was shown for the pristine and modified ZrO_2 ceramics during a short time modification (5h). For a longer modification time the results are presented in Fig. S7. In the right-upper part of the Kao diagram, samples possessing a hydrophilic or highly hydrophilic character are located, irrespective of the surface roughness. The non-modified ZrO_2 membrane is placed in that part. Furthermore, in the first quarter of the coordinate system, the modified surfaces wetted by solvents with low liquid surface tension are also located (i.e., ethyl iodide, butyl acetate, methyl tert-butyl ether, perfluorohexane, and n-hexane). Taking into account the chosen testing liquids, evaluated roughness parameter and wetting behaviour (i.e. critical surface tension, spreading pressure and sliding angle), it was possible to foresee the wettability of the evaluated ceramic membranes. Concerning the results for water as a testing liquid, it can be stated that 5kD functionalized surfaces are mostly located in the Wenzel region (Fig. 7). However, the more open structure of 300kD, that was modified with higher effectiveness (Figs. 1 and S2), and characterized by higher CA and roughness are placed in both Wenzel as well as Cassie-Baxter region of the Kao diagram. For the highly hydrophobic heterogenic surface, air pockets locked in the asperity valleys will be noted (for 5kD-FC12 and 300kD-FC12 after 2nd grafting and for all samples after 3rd modification). Consequently, it will be possible to form a composite solid–liquid-air interface and to raise the value of CA. It needs to be highlighted that the achieved experimental data from the material analysis are in good accordance with the literature findings [14,17,58]. Interesting results were established for FC6 and FC12 showing the best water resistance (location in the Cassie-Baxter region – Fig. 7, Fig. S7). Also, these data proved that it is possible to use molecules with shorter carbon chains to generate more hydrophobic and water-resistant material, irrespective of the morphology of the starting material. Finally, it is a promising way to prepare highly hydrophobic material applying a fluorine-free analogue of the grafting agent (Fig. 7). 300kD ceramic treated with C6 was placed in the Cassie-Baxter zone. These findings are valuable for the potential applications and commercialization, e.g., generation of highly specialized materials with predictable surface features. To conclude, the modification process with fluorinated and fluorine-free molecules was quite considerably efficient and changed both the ceramic morphology and the physicochemical properties.

3.4. Impact of functionalization process on mechanical features

Besides the wettability behaviour of the modified material, an essential issue was to define its stability. The features were introduced as the correlation between work of adhesion (W_a) and adhesive force (F_a) as well as nanohardness (H_n) and elasticity index (H/E) (Figs. 9 and 10). Equilibrium of adhesion work is a parameter on which the wettability, as well as mechanical features, has an essential impact from the thermodynamic point of view [9, 56]. This is because of the generation and elimination of interfacial areas that cause changes in reversible free energy. In the course of AFM measurements, the F_a acting in ambient environments among the substrate (i.e., ceramic) and AFM probe is typically brought up to originate mostly from the destruction and distortion of the capillary bridges between the surface and tip [9,56]. Frequently, these bridges initiate from the condensates of water vapours that naturally pledge at structural indiscretions, e.g., cracks or pore. Heterogeneities of the surface in nano and/or micro-scale, can let water penetrate through the irregularities and as a final point generate nano- or microdroplets, even on the highly hydrophobic/hydrophilic sample [56,59]. Such behaviour has been found for all investigated ZrO_2 ceramic samples grafted with perfluorinated and fluorine-free

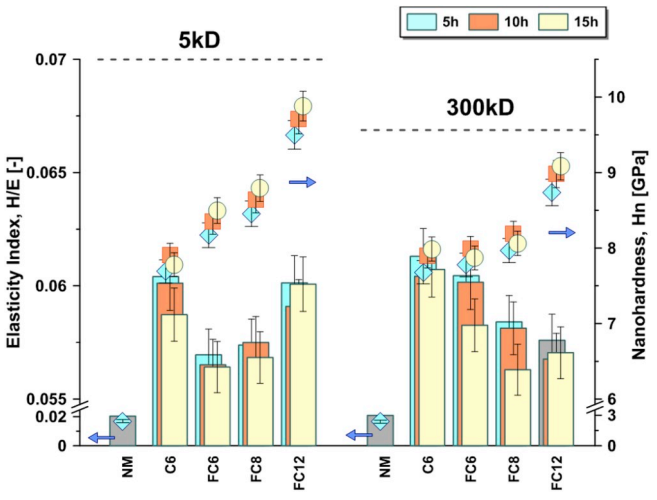

Fig. 9. Mechanical stability of modified membranes – evolution of elasticity index and nanohardness.

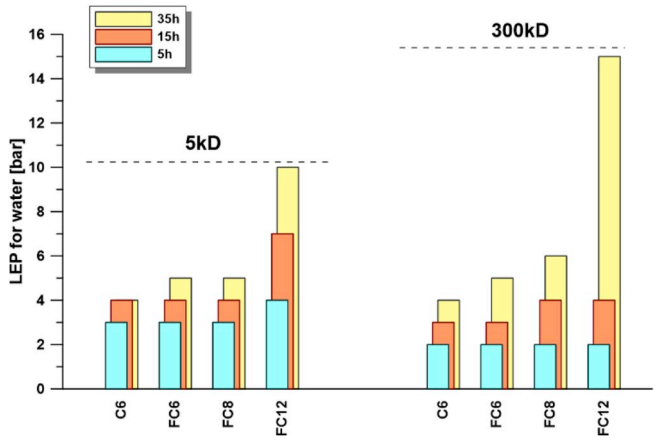

Fig. 10. Grafting efficacy of cylindrical ZrO_2 membranes.

molecules, presenting the RMS values in the range of 6.58 nm–45.12 nm. Concerning the capillary forces, having their nature independent from the chemistry of surface structure, a significant influence on the measured adhesive force was observed.

In Fig. 8, local adhesive features are presented as an evaluation of F_a with microscopic F_a for the water-ceramic system. The diminution of adhesive features was noted as a consequence of ZrO_2 ceramic modification, both with fluorinated and non-fluorinated molecules (Figs. 2 and 4). The values of F_a and W_a were equal to 25.2 ± 1.0 nN and 128.8 ± 3.8 mN m^{-1} for 5kD and 29.5 ± 1.1 nN and 134.1 ± 4.0 mN m^{-1} for 300kD, respectively. As an effect of functionalization, the significant decrease of work of adhesion and F_a was found with a rise of the length of the grafting agents as well as an extension of grafting time. F_a after treatment with silanes modifiers was in the range of 2.1 ± 0.1 nN and 6.2 ± 0.2 nN depending on the duration of grafting and grafting agent type. The modifiers possessing longer chains are considered to be better antiadhesive agents. However, the values of W_a were in the range of 11.1 ± 0.3 mN m^{-1} and 56.4 ± 1.7 mN m^{-1} (Fig. 8). It was noted that for capillary condensation occurrence, the measured F_a is subjected to surface chemistry. Out of that, the dispersive and capillary interaction can affect the value of F_a [60,61]. Although practically linear relation has been noted between F_a and W_a of modified ceramics, a slightly different trend has been observed for samples modified with FC12 (Fig. 8). In that case, the pore size of the membrane becomes important. In the case of 5kD, the experimental points for FC12 were far from the linear correlation with other points (Fig. 8A). For 300kD ceramics, not only the higher reduction of F_a but also stronger impact on grafting molecules has been found. Values of adhesion work for 300kD were smaller in the comparison to 5kD owing to the higher hydrophobicity level (Fig. 3). An analogous relationship between W_a and F_a was presented by Bhushan et al. [62] during the formation of the self-assembly monolayers from biphenyl thiol and alkylthiol possessing various reactive groups. It was stated that film made from hexadecane thiol with a methyl terminal group presented the lowest frictional force and the adhesive force because of its low W_a and its highly acquiescent long carbon chain. Bhushan et al. [62] also explained that the creation of water capillary could impact F_a. Furthermore, the intensive study about the relationship between W_a and F_a was described by Psarski et al. [56] who worked with a coating of glass and silicon by various perfluoroalkylsilanes possessing between 1 and 8 carbon atoms in fluorocarbon chain.

Modification with the mentioned modifiers improved the mechanical properties. The hardness of the samples increased from 2.41 GPa (5kD-NM), 2.36 GPa (300kD-NM), up to a range of 7.68 ± 0.23 GPa (5kD-C6 5h) and 9.88 ± 0.29 GPa (300kD-FC12 35h). Contrary to the modulation of hydrophobicity level, by the selection of specific molecules and subsequently influencing not only CA (Fig. 3) but also roughness (Fig. 5), an increase in the number of carbon chains in grafting molecules results in an improvement in nanohardness (Fig. 9). Moreover, the existence of fluorine has a noticeable impact. The time of modification, however, has an only marginal influence on the hardness of ceramics. Inversely to the observed tendency of hardness parameter, the elasticity index (H/E) is reduced with the length of the carbon-chain. Nevertheless, the impact of a grafting agent is seen. The elasticity index for pristine ceramics was equal to 0.0203 (5kD-NM) and 0.0209 (300kD-NM), respectively. As an effect of hydrophobization, that parameter changed to 0.0564–0.0604 for 5kD samples and 0.0559 to 0.0613 for 300kD membranes, accordingly. That remark is related to the fact that H_n/E depends on both H_n as well as on the Young modulus (E). The gathered data of mechanical features are in close relation with the adhesion properties (Fig. 8). The high value of elasticity index for C6 membranes was related to the higher value of Young modulus. This remark has an essential meaning for the generation of highly, mechanically resistant membranes. The findings showed that the presence of fluorine has an important influence the mechanical features.

The determined values of tribological factors are in good accordance with the literature data [63]. The Young modulus for the zirconia material can be varied between 105 – 225 GPa and depends on the porosity, method of preparation of the material (e.g. classical sintering at 1110°C or spark plasma sintering), and existence of additives (e.g. yttria used for stabilization) [64]. The noted variations in data of H_n and E in the presented research can be explained by the greater stiffness of the fluorocarbon chains. The Young modulus for the pristine investigated membranes was equal to 118.3 ± 4.7 GPa (5kD-NM) and 127.3 ± 5.0 GPa (300kD-NM), respectively. After the treatment these values changed as follows 127.3 ± 3.8 GPa (5kD-C6 5h) – 164.4 ± 4.9 GPa (5kD-FC12 35h), and 125.3 ± 3.7 GPa (300kD-C6 5h) – 159.3 ± 4.7 GPa (300kD-C6 5h). Moreover, this can be linked to a turning of the structure of perfluorinated molecules that is significantly smaller in the comparison of non-fluorinated modifiers. It is related to the smaller size of hydrogen atoms compared with fluorine [65]. The generated nanolayer of alkylsilane is less stiff than the fluorinated one. For this reason, carbons can easily move without hindrance compared to molecules of perfluorinated modifiers [66]. Comparable results were shown by Bhushan et al. [62,65]. It was presented that for a self-assembled monolayer possessing a backbone structure with greater stiffness, more energy is required for the elastic distortion. That enlightenment can help to understand why the smaller values of H and E were found for ZrO_2 samples functionalized with fluorine-free grafting agents (Fig. 9) [62,65].

3.5. *The separation efficiency of modified ceramics in the desalination process by applying AGMD process*

Successfully hydrophobized zirconia membranes were subsequently characterized in the desalination process of NaCl aqueous solutions by employing the air-gap membrane distillation process (AGMD). The AGMD configuration has been selected owing to their advantage of heat loss reduction by the membrane material owing to the presence of air gap and the possibility of getting higher permeate flux. The heat transfer in AGMD is a complex feature including many variables i.e. transfer of heat through the feed boundary layer, through membrane and the gas gap, the condensation phenomenon at the cold surface, as well as the transfer of heat through the condensate liquid boundary layer and to the cooling water. The selection of ZrO_2 materials was beneficial because of their low value of thermal conductivity [67]. In the above-mentioned parts, it was presented that zirconia membranes meet all the necessities of the MD process, i.e., there are hydrophobic, porous, and resistant to wetting [68,69]. The strong hydrophobic character was proved by CA (Fig. 3) and a high LEP value for water (Fig. 10). Moreover, the theoretical lack of wetting was confirmed by critical surface tension established basing the Zisman method and plotted on the Kao diagram as well. Application of shorter molecules gave a gradual increase in the LEP

value (Fig. 10), however utilization of FC12 caused the partial pore blocking of the membrane. This remark was supported by the observed highest LEP pressure for both 5kD and 300kD membranes after 15h and 35h of grafting.

As a first step before the separation process, membranes were tested only in contact with pure water as feed. Transport of water, as well as the separation process, was accomplished with an applied driving force equal to 689 mbar [70]. Transport of vapours of solvent (i.e., water) in MD can be described as follows (Eqs. (8) and (9)) [71]:

$$J_{H2O} = K(p_f - p_p) \quad 8$$

$$K = \left[\frac{1}{K_f} + \frac{1}{K_m} + \frac{1}{K_p}\right]^{-1} \quad 9$$

where: K – overall mass transfer coefficient [kg $m^{-2}s^{-1}Pa^{-1}$], p_f – partial vapour pressure of water in feed, p_p – partial vapour pressure of water in permeate; K_f – mass transfer coefficient of feed layer, K_m – mass transfer coefficient of membrane and K_p – mass transfer coefficient of permeate layer.

K parameter depends roughly on the membrane properties, e.g., thickness, pore size, porosity, type of material, morphology, and tortuosity [72]. Despite the fact that mass transfer coefficient K is related to the temperature and pressure values, commonly, its value is almost constant [72]. This was seen for the zirconia membranes decorated with silane-based modifiers (Table 1).

For the determination of water vapour pressure Bulk's equation (Eq. (10)) was implemented owing to the fact that is a more accurate approach in comparison with Antoine's equation [73].

$$P = 0.61121 exp\left[\left(18.678 - \frac{T}{234.5}\right)\left(\frac{T}{257.14 + T}\right)\right] \quad 10$$

where temperature (T) is in [°C], and pressure (P) is in [kPa].

With regards to the data gathered in Table 1, a slight influence of the type of silane-based modifier and pore size of the membrane was noted. Furthermore, a visible impact of grafting time was also observed. The decrease of overall mass transfer coefficient with the extension of modification time was associated with the higher hydrophobicity level and subsequently with less favourable water transport crosswise the ceramic membrane. Membranes decorated with C6 possessed the highest values of the K parameter. Conversely, the smallest mass transfer coefficient was found for ZrO_2 membranes modified using FC12, however only for the second and the third grafting. This observation can be related to the partial clogging of pores by grafting molecules, principally for the 5kD membrane. It that case the size of grafting molecules (≈ 2.2 nm) was similar to the pore size of the membrane (3 nm). The higher value of water permeates as well as K factor for 5kD-FC12 membrane treated 5h can be related to smaller density of the attachment of the molecules.

Table 1
Overall mass transfer coefficient for the investigated membranes.

Membrane	J_{H2O} [kg m^{-2} h^{-1}]	K [kg m^{-2} s^{-1} Pa^{-1}]	J_{H2O} [kg m^{-2} h^{-1}]	K [kg m^{-2} s^{-1} Pa^{-1}]	J_{H2O} [kg m^{-2} h^{-1}]	K [kg m^{-2} s^{-1} Pa^{-1}]
	1st modification – 5h		2nd modification – 15h		3rd modification – 35h	
5kD-C6	3.66	1.47 10^{-8}	2.45	0.98 10^{-8}	1.29	0.52 10^{-8}
5kD-FC6	3.05	1.22 10^{-8}	2.04	0.82 10^{-8}	1.08	0.43 10^{-8}
5kD-FC8	2.73	1.10 10^{-8}	1.50	0.60 10^{-8}	0.67	0.27 10^{-8}
5kD-FC12	1.08	0.43 10^{-8}	0.00	–	0.00	–
300kD-C6	4.56	1.83 10^{-8}	3.01	1.21 10^{-8}	2.40	0.96 10^{-8}
300kD-FC6	3.80	1.52 10^{-8}	2.51	1.01 10^{-8}	2.00	0.81 10^{-8}
300kD-FC8	3.77	1.51 10^{-8}	2.42	0.97 10^{-8}	1.72	0.67 10^{-8}
300kD-FC12	4.16	1.67 10^{-8}	1.91	0.76 10^{-8}	0.00	–

The established data on transport properties for pure water and salty water were presented together in Fig. 11. The influence of membrane morphology, grafting agent (Fig. 11A and B), as well as time of modification (Fig. 11 A1-A3; B1-B3) on the transport features, has been evaluated. It was proved that all these factors influence water transport through ZrO_2 ceramic membranes. Firstly, the observed changes can be related to the differences in the tortuosity of the membrane pores and pore diameter after the grafting processes as well as related to the LEP values (Figs. 1, 2 and 9). 300kD membranes possessed higher permeate fluxes compare to 5kD membranes, which is clearly associated with their morphology, i.e., bigger pore size diameter, higher porosity, and lower LEPw value. Consequently, the mechanism of vapours transport will be different for 5kD and 300kD membranes [37,74]. The extension of modification time from 5h to 35h causes a significant reduction of the permeate flux (Fig. 11). Moreover, the type of grafting agents appears to have an important influence on the transport properties. The highest fluxes were noted for membranes grafted with a non-fluorinated agent (C6).

The utilization of C6 makes it possible to generate hydrophobic membranes (Figs. 2 and 9) characterized by excellent water repellence (Figs. 5 and 6) with improved permeability. Membrane treated with C6 show a slightly lower contact angle for water (Fig. 3) and roughness (Fig. 5) which gave water molecules easier access through the ceramic structure. Moreover, fluorine free membranes were more stable towards hexane treatment under sonication (Table S1). Furthermore, the lower spreading pressure and higher critical surface tension (Figs. 6 and 7) ensure higher affinity to water as well. This was associated with the stronger polar interaction with the functionalized ceramic material. Production of the fluorine-free materials has a huge application potential e.g. food and water industries, where possible fluorine toxicity should be avoided. The reduction of transport features was also observed with the increase of NaCl feed solution concentration. This fact is associated with the decrease in driving force during the MD process with the feed possessing more non-vapour species. The mentioned observation can be elucidated by the Raoult's law stating that the vapour pressure above the solution containing more non-volatile component is diminished [74]. Taking into account the type of modifiers, it can be seen that the type of perfluorinated molecules has also a significant influence on the permeate flux. The less permeable membrane was that modified with FC12 molecules (Fig. 11). This observation can be associated with a mode of PFAS chain anchoring inside the porous structure membrane followed by a rise of membrane tortuosity and subsequently influencing LEP value (Fig. 10). In addition, the partial pores clogging by perfluoroalkylsilanes is also possible [75].

This was observed for 5kD-FC12 treated during 15h (Fig. 11 A2) and 35h (Fig. 11 A3) as well as for 35h-grafted membrane 300kD-FC12 (Fig. 11 B3). The retention coefficient of salt (R_{NaCl}) (Eq. (1)) is a significant factor determining the efficacy of the desalination process. From the theoretical point of view, this value should be equal to 100% owing to the fact that only vapours of the solvent can be transported through the porous hydrophobic material. The gathered data are in good accordance with that theoretical statement (Fig. 13). For all the investigated samples high level of salt rejection (~99%) was observed. Moreover, no influence of membrane character, time of modification as well as type of grafting agent was found (Fig. 13). Out of the received data, it can be stated that no wetting took place during the separation. It was also proved by the observed stable flux of permeate during the AGMD process (Fig. 12). In comparison with the literature data, an upgrading of membrane performance was seen (Table 2). For example

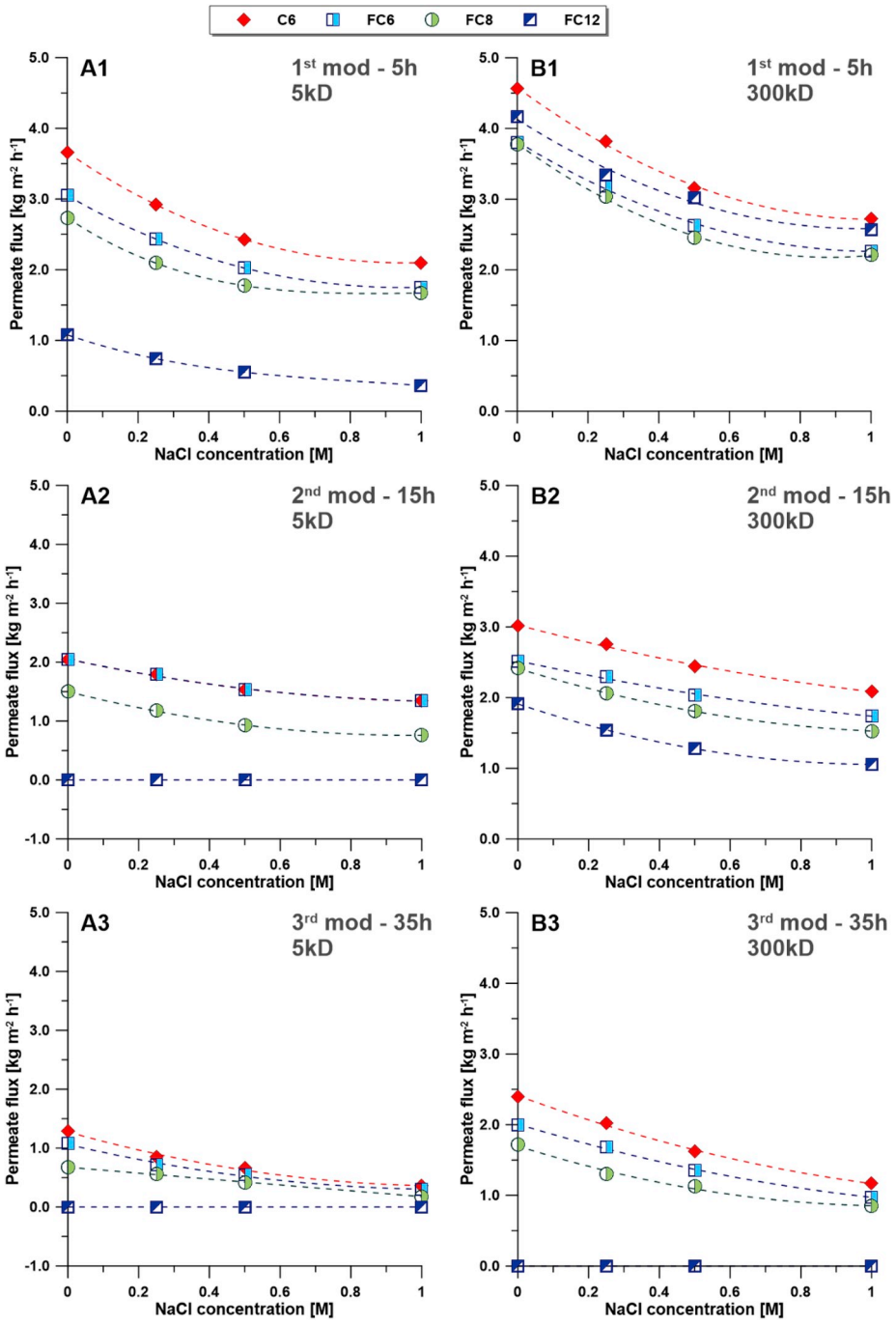

Fig. 11. Transport properties of the modified ZrO_2 membranes 5kD (A) and 300kD (B) during 5h (A1, B1), 15h (A2, B2) and 35h (A3, B3).

Krajewski and co-workers [34] used ZrO_2-200nm membranes for desalination of 0.1 gL^{-1} NaCl in AGMD. The reported values of permeate flux were around 6 $kg\,m^{-2}\,h^{-1}$. However, the driving force was much higher than in our case of ca. 30%. Liu et al. [35] tested a zirconia membrane stabilized by yttria, however the membrane has a very open structure with pore size of ca. 1 μm.

As a result of such open structure very high flux was noted ca. 28.7 $kg\,m^{-2}\,h^{-1}$. Chen and co-workers [7] presented interesting membrane based on alumina (150 nm) and modified with a long fluorine-free alkyl chain possessing 16 atoms. The membrane was used for the desalination of 30 gL^{-1} NaCl in VMD. Owing to the different driving force in vacuum MD, the high permeate flux was noted equal to 30 $kg\,m^{-2}\,h^{-1}$, however the membrane was not stable in a long-lasting process. Modification of the ceramic membrane with carbon nanotubes gave a chance to improve the transport properties due to the presence of carbon-based materials and very open porous structure (pore size 470 nm) promoted water transport [76]. The membranes were very stable and superhydrophobic (CA = 168°) characterized by permeate flux of 25.3 $kg\,m^{-2}\,h^{-1}$ during the desalination process of 70gL^{-1} NaCl in electrochemically assisted direct contact MD.

4. Conclusions

To improve the membrane separation process, it is necessary to comprehend the process from the viewpoint of the membrane material, e.g., its chemistry and material features. The molecular grafting of zirconia ceramic membranes was successfully accomplished to turn the natural hydrophilic character of the ceramics to a highly hydrophobic

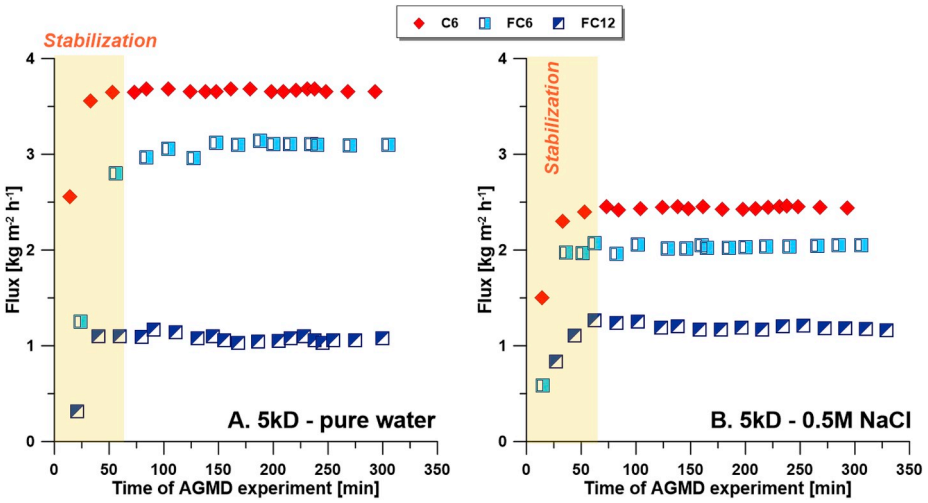

Fig. 12. Evolution of permeate flux for selected 5kD membranes modified 5h with C6, FC6 and FC12. Feed solutions: water (A) and 0.5 M NaCl (B).

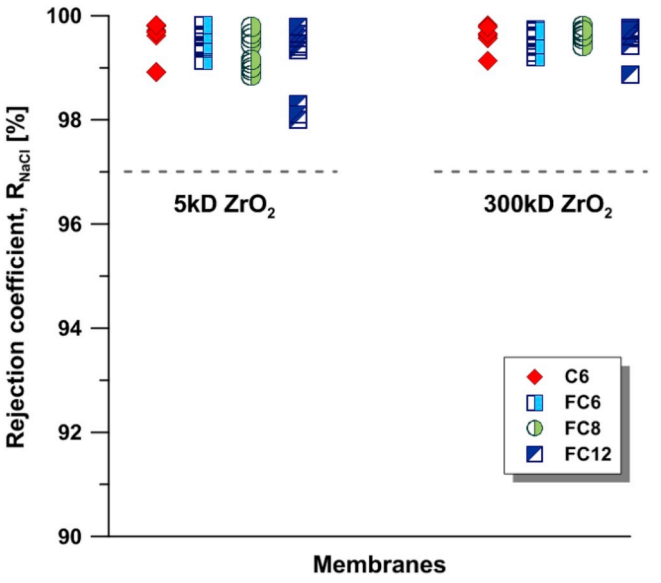

Fig. 13. Separation properties of the investigated ceramic membranes.

one. The prepared membranes were highly resistant to water, possessed a raised hydrophobicity level and for this reason were suitable for the membrane distillation process. All membranes were efficiently modified, and the contact angle increased from ca. 40° to 105–148° depending the employed experimental conditions. An intensive material and physicochemical characterization has been carried out. Contact and sliding angle, roughness parameter, t-plot, and adhesive features (work of adhesion and adhesive force) were determined to assess how the modification (a type of grafting agent and length of time of modification) influence material properties. Furthermore, spreading pressure, critical surface tension (Zisman plot method) and Kao diagram were implemented to evaluate wetting ability. Mechanical stability was determined by description nanohardness, Young modulus, and elasticity index. The established parameters were referred to the membrane separation effectiveness in desalination air-gap membrane distillation. The calculated and achieved data from material analyses suits well with the experimental data from MD tests. No wetting has been observed during the course of desalination process that was in good accordance with determined critical surface tension and Kao diagram. Although the modification time did not influence many material properties, the impact on transport features was clearly visible, especially for membranes treated with FC12. Owing to the long molecules and high fluorination degree, ceramic membranes with both morphologies (5kD and 300kD) suffered from pore-clogging and severe flux reduction. The most

Table 2
Comparison of ceramic and polymeric membranes performance.

Membrane material	MD Process	Pore size/porosity	CA [deg]	Temp feed [°C]	Feed	Flux [kg m^{-2} h^{-1}]	Ref.
Al_2O_3-FDTS	DCMD	80 nm, 32%	150	70	0.7 M NaCl	7.2	[25]
		160 nm 57%	161			8.2	
SiO_2 ceramic with Si_2N_2O nanowires	SGMD	0.81 μm, 49%	160	90	4% NaCl	11.11	[27]
Al_2O_3 –C16	VMD	150 nm	161	70	30 gL^{-1} NaCl	30	[7]
CNT-ceramic	e-DCMD	0.47 μm	168	80	70 gL^{-1}	25.3	[76]
Al_2O_3-FAS	VMD	0.40 μm	158	70	3.5 wt% NaCl	29.3	[19]
Si_3N_4	SGMD	0.81 μm, 57%	–	75	3.5 wt% NaCl	11.75	[77]
γ-$Y_2Si_2O_7$	SGMD	0.9 μm, 49%	132	90	20 wt% NaCl	10.03	[78]
ZrO_2-YSZ	DCMD	4.5 μm, 43%	135	80	2 wt% NaCl	28.7	[35]
Al_2O_3	AGMD	100 nm	132	90	0.25 wt% NaCl	3.7	[79]
TiO_2		75 nm	128			1.9	
ZrO_2	AGMD	200 nm	142	95	0.1 gL^{-1}	6	[34]
PVDF	DCMD	0.21 μm, 53%	135	50	3.5 wt% NaCl	21	[80]

C16 - hexadecyltrimethoxysilane.
FDTS- perfluorodecyltrichlorosilane.
e-DCMD - electrochemically assisted direct contact MD.
FAS - 1H,1H,2H,2H-Perfluorodecyltriethoxysilane.
PFAS-1H,1H,2H,2H-perfluorooctyltrichlorosilane.

important and interesting finding was the fact that the utilization of non-fluorinated modifiers can be more suitable for highly permeable ceramics, possessing excellent transport and separation properties as well as mechanical stability. Membrane 300kD grafted 5h with C6 had more than 20% better transport features and comparable material properties than FC6 modified in the same modification conditions. Measured permeate fluxes during the desalination of 0.5 M NaCl for 300kD-C6 sample were equal to 3.15 $kg\,m^{-2}\,h^{-1}$ and 2.63 $kg\,m^{-2}\,h^{-1}$ for 300kD-FC6. Furthermore, 300kD-C6 membrane was characterized by $CA = 114°$, $R_q = 33.58 \pm 1.01$ nm, and critical surface tension 20.4 ± 0.6 $mN\,m^{-1}$. The same parameters for 300kD sample modified with fluorinated analogue as followed, $CA = 110°$, $R_q = 35.72 \pm 1.07$ nm, and critical surface tension 19.2 ± 0.5 $mN\,m^{-1}$, respectively.

Declaration of competing interest

None.

Acknowledgment

This research was supported by 2017/26/D/ST4/00752 (Sonata 13) grant from the National Science Centre Poland, Poland. Partially research was supported by the statutory funds of Nicolaus Copernicus University in Toruń, Poland (Faculty of Chemistry T-109 "Membranes and membrane separation processes - fundamental and applied research").

Appendix A. Supplementary data

Supplementary data to this article can be found online at https://doi.org/10.1016/j.memsci.2019.117597.

References

[1] A.T. Servi, J. Kharraz, D. Klee, K. Notarangelo, B. Eyob, E. Guillen-Burrieza, A. Liu, H.A. Arafat, K.K. Gleason, A systematic study of the impact of hydrophobicity on the wetting of MD membranes, J. Membr. Sci. 520 (2016) 850–859.
[2] J. Swaminathan, H.W. Chung, D.M. Warsinger, F.A. AlMarzooqi, H.A. Arafat, J. H. Lienhard V, Energy efficiency of permeate gap and novel conductive gap membrane distillation, J. Membr. Sci. 502 (2016) 171–178.
[3] M. Rezaei, D.M. Warsinger, J.H. Lienhard V, M.C. Duke, T. Matsuura, W. M. Samhaber, Wetting phenomena in membrane distillation: mechanisms, reversal, and prevention, Water Res. 139 (2018) 329–352.
[4] D. Woldemariam, A. Kullab, U. Fortkamp, J. Magner, H. Royen, A. Martin, Membrane distillation pilot plant trials with pharmaceutical residues and energy demand analysis, Chem. Eng. J. 306 (2016) 471–483.
[5] N. Thomas, M.O. Mavukkandy, S. Loutatidou, H.A. Arafat, Membrane distillation research & implementation: lessons from the past five decades, Separ. Purif. Technol. 189 (2017) 108–127.
[6] A. Hussain, A. Seidel-Morgenstern, E. Tsotsas, Heat and mass transfer in tubular ceramic membranes for membrane reactors, Int. J. Heat Mass Transf. 49 (2006) 2239–2253.
[7] X. Chen, X. Gao, K. Fu, M. Qiu, F. Xiong, D. Ding, Z. Cui, Z. Wang, Y. Fan, E. Drioli, Tubular hydrophobic ceramic membrane with asymmetric structure for water desalination via vacuum membrane distillation process, Desalination 443 (2018) 212–220.
[8] L.-Z. Zhang, Q.-W. Su, Performance manipulations of a composite membrane of low thermal conductivity for seawater desalination, Chem. Eng. Sci. 192 (2018) 61–73.
[9] L. Gao, T.J. McCarthy, Teflon is hydrophilic. Comments on definitions of hydrophobic, shear versus tensile hydrophobicity, and wettability characterization, Langmuir 24 (2008) 9183–9188.
[10] M.P. Krafft, J.G. Riess, Chemistry, physical chemistry, and uses of molecular Fluorocarbon−Hydrocarbon diblocks, triblocks, and related compounds—unique “apolar” components for self-assembled colloid and interface engineering, Chem. Rev. 109 (2009) 1714–1792.
[11] J. Osés, G. Fuentes, J. Palacio, J. Esparza, J. García, R. Rodríguez, Antibacterial functionalization of PVD coatings on ceramics, Coatings 8 (2018) 197.
[12] P. Wang, T.-S. Chung, Recent advances in membrane distillation processes: membrane development, configuration design and application exploring, J. Membr. Sci. 474 (2015) 39–56.
[13] B. Khorshidi, I. Biswas, T. Ghosh, T. Thundat, M. Sadrzadeh, Robust fabrication of thin film polyamide-TiO(2) nanocomposite membranes with enhanced thermal stability and anti-biofouling propensity, Sci. Rep. 8 (2018) 784.
[14] A.B.D. Cassie, S. Baxter, Wettability of porous surfaces, Trans. Faraday Soc. 40 (1944) 546–551.
[15] L. Eykens, K. De Sitter, C. Dotremont, W. De Schepper, L. Pinoy, B. Van Der Bruggen, Wetting resistance of commercial membrane distillation membranes in waste streams containing surfactants and oil, Appl. Sci. 7 (2017) 118.
[16] Y. Ibrahim, H.A. Arafat, T. Mezher, F. AlMarzooqi, An integrated framework for sustainability assessment of seawater desalination, Desalination 447 (2018) 1–17.
[17] K.J. Kubiak, M.C.T. Wilson, T.G. Mathia, P. Carval, Wettability versus roughness of engineering surfaces, Wear 271 (2011) 523–528.
[18] D.M. Warsinger, A. Servi, G.B. Connors, M.O. Mavukkandy, H.A. Arafat, K. K. Gleason, J.H. Lienhard V, Reversing membrane wetting in membrane distillation: comparing dryout to backwashing with pressurized air, Environ. Sci.: Water Res. Technol. 3 (2017) 930–939.
[19] C.-Y. Huang, C.-C. Ko, L.-H. Chen, C.-T. Huang, K.-L. Tung, Y.-C. Liao, A simple coating method to prepare superhydrophobic layers on ceramic alumina for vacuum membrane distillation, Separ. Purif. Technol. 198 (2018) 79–86.
[20] J. Kujawa, S. Al-Gharabli, W. Kujawski, K. Knozowska, Molecular grafting of fluorinated and nonfluorinated alkylsiloxanes on various ceramic membrane surfaces for the removal of volatile organic compounds, Appl. Vac. Membr. Distillc. 9 (2017) 6571–6590.
[21] J. Kujawa, S. Cerneaux, W. Kujawski, M. Bryjak, J. Kujawski, How to functionalize ceramics by perfluoroalkylsilanes for membrane separation process? Properties and application of hydrophobized ceramic membranes, ACS Appl. Mater. Interfaces 8 (2016) 7564–7577.
[22] M. Shaban, A.M. Ashraf, H. AbdAllah, H.M. Abd El-Salam, Titanium dioxide nanoribbons/multi-walled carbon nanotube nanocomposite blended polyethersulfone membrane for brackish water desalination, Desalination 444 (2018) 129–141.
[23] S.K. Hubadillah, M.H.D. Othman, A.F. Ismail, M.A. Rahman, J. Jaafar, A low cost hydrophobic kaolin hollow fiber membrane (h-KHFM) for arsenic removal from aqueous solution via direct contact membrane distillation, Separ. Purif. Technol. 214 (2019) 31–39.
[24] M. Friedrich, M. Seiler, S. Waechter, J. Bliedtner, J.P. Bergmann, Precision structuring and functionalization of ceramics with ultra-short laser pulses, J. Laser Appl. 30 (2018), 032501.
[25] N. Subramanian, A. Qamar, A. Alsaadi, A. Gallo, M.G. Ridwan, J.-G. Lee, S. Pillai, S. Arunachalam, D. Anjum, F. Sharipov, N. Ghaffour, H. Mishra, Evaluating the potential of superhydrophobic nanoporous alumina membranes for direct contact membrane distillation, J. Colloid Interface Sci. 533 (2019) 723–732.
[26] Y. Yang, Q. Liu, H. Wang, F. Ding, G. Jin, C. Li, H. Meng, Superhydrophobic modification of ceramic membranes for vacuum membrane distillation, Chin. J. Chem. Eng. 25 (2017) 1395–1401.
[27] L. Li, H. Abadikhah, J.-W. Wang, X. Xu, S. Agathopoulos, One-step synthesis of flower-like Si2N2O nanowires on the surface of porous SiO2 ceramic membranes for membrane distillation, Mater. Lett. 232 (2018) 74–77.
[28] M.I. Siyal, A.A. Khan, C.-K. Lee, J.-O. Kim, Surface modification of glass fiber membranes by fluorographite coating for desalination of concentrated saline water with humic acid in direct-contact membrane distillation, Separ. Purif. Technol. 205 (2018) 284–292.
[29] S. Ali, S.A.U. Rehman, H.-Y. Luan, M.U. Farid, H. Huang, Challenges and opportunities in functional carbon nanotubes for membrane-based water treatment and desalination, Sci. Total Environ. 646 (2019) 1126–1139.
[30] S.K. Hubadillah, M.H.D. Othman, T. Matsuura, M.A. Rahman, J. Jaafar, A.F. Ismail, S.Z.M. Amin, Green silica-based ceramic hollow fiber membrane for seawater desalination via direct contact membrane distillation, Separ. Purif. Technol. 205 (2018) 22–31.
[31] A. Politano, P. Argurio, G. Di Profio, V. Sanna, A. Cupolillo, S. Chakraborty, H. A. Arafat, E. Curcio, Photothermal membrane distillation for seawater desalination, Adv. Mater. 29 (2017) 1603504.
[32] A.V. Dudchenko, C. Chen, A. Cardenas, J. Rolf, D. Jassby, Frequency-dependent stability of CNT Joule heaters in ionizable media and desalination processes, Nat. Nanotechnol. 12 (2017) 557.
[33] R. Rasouli, A. Barhoum, H. Uludag, A review of nanostructured surfaces and materials for dental implants: surface coating, patterning and functionalization for improved performance, Biomater. Sci. 6 (2018) 1312–1338.
[34] S.R. Krajewski, W. Kujawski, M. Bukowska, C. Picard, A. Larbot, Application of fluoroalkylsilanes (FAS) grafted ceramic membranes in membrane distillation process of NaCl solutions, J. Membr. Sci. 281 (2006) 253–259.
[35] T. Liu, L. Lei, J. Gu, Y. Wang, L. Winnubst, C. Chen, C. Ye, F. Chen, Enhanced water desalination performance through hierarchically-structured ceramic membranes, J. Eur. Ceram. Soc. 37 (2017) 2431–2438.
[36] J. Kujawa, W. Kujawski, S. Koter, K. Jarzynka, A. Rozicka, K. Bajda, S. Cerneaux, M. Persin, A. Larbot, Membrane distillation properties of TiO_2 ceramic membranes modified by perfluoroalkylsilanes, Desalin. Water Treat. 51 (2013) 1352–1361.
[37] W. Kujawski, J. Kujawa, E. Wierzbowska, S. Cerneaux, M. Bryjak, J. Kujawski, Influence of hydrophobization conditions and ceramic membranes pore size on their properties in vacuum membrane distillation of water–organic solvent mixtures, J. Membr. Sci. 499 (2016) 442–451.
[38] J. Kujawa, W. Kujawski, A. Cyganiuk, L.F. Dumée, S. Al-Gharabli, Upgrading of zirconia membrane performance in removal of hazardous VOCs from water by surface functionalization, Chem. Eng. J. 374 (2019) 155–169.
[39] J. Kujawa, S. Cerneaux, W. Kujawski, Removal of hazardous volatile organic compounds from water by vacuum pervaporation with hydrophobic ceramic membranes, J. Membr. Sci. 474 (2015) 11–19.
[40] D.Y. Kwok, A.W. Neumann, Contact angle measurement and contact angle interpretation, Adv. Colloid Interface Sci. 81 (1999) 167–249.

[41] W.A. Zisman, Relation of the equilibrium contact angle to liquid and solid constitution, in: Contact Angle, Wettability, and Adhesion, American Chemical Society, 1964, pp. 1–51.
[42] A. Lecloux, J.P. Pirard, The importance of standard isotherms in the analysis of adsorption isotherms for determining the porous texture of solids, J. Colloid Interface Sci. 70 (1979) 265–281.
[43] W. Li, A. Amirfazli, A thermodynamic approach for determining the contact angle hysteresis for superhydrophobic surfaces, J. Colloid Interface Sci. 292 (2005) 195–201.
[44] C. Scherdel, G. Reichenauer, M. Wiener, Relationship between pore volumes and surface areas derived from the evaluation of N2-sorption data by DR-, BET- and t-plot, Microporous Mesoporous Mater. 132 (2010) 572–575.
[45] W.R. Purcell, Interpretation of Capillary Pressure Data, 1950. SPE-950369-G.
[46] G.M. Dorris, D.G. Gray, Adsorption, spreading pressure, and london force interactions of hydrocarbons on cellulose and wood fiber surfaces, J. Colloid Interface Sci. 71 (1979) 93–106.
[47] T. Onda, S. Shibuichi, N. Satoh, K. Tsujii, Super-water-repellent fractal surfaces, Langmuir 12 (1996) 2125–2127.
[48] R.N. Wenzel, Resistance of solid surfaces to wetting by water, Ind. Eng. Chem. Res. 28 (1936) 988–994.
[49] M. Thommes, K. Kaneko, V. Neimark Alexander, P. Olivier James, F. Rodriguez-Reinoso, J. Rouquerol, S.W. Sing Kenneth, Physisorption of gases, with special reference to the evaluation of surface area and pore size distribution (IUPAC Technical Report). Pure and Applied Chemistry, 2015, p. 1051.
[50] L. Matějová, O. Šolcová, P. Schneider, Standard (master) isotherms of alumina, magnesia, titania and controlled-pore glass, Microporous Mesoporous Mater. 107 (2008) 227–232.
[51] P. Schneider, Adsorption isotherms of microporous-mesoporous solids revisited, Appl. Catal., A 129 (1995) 157–165.
[52] T. Van Gestel, H. Kruidhof, D.H.A. Blank, H.J.M. Bouwmeester, ZrO_2 and TiO_2 membranes for nanofiltration and pervaporation: Part 1. Preparation and characterization of a corrosion-resistant ZrO_2 nanofiltration membrane with a MWCO < 300, J. Membr. Sci. 284 (2006) 128–136.
[53] E. Bystrzycka, M. Prowizor, I. Piwoński, A. Kisielewska, D. Batory, A. Jędrzejczak, M. Dudek, W. Kozłowski, M. Cichomski, The effect of fluoroalkylsilanes on tribological properties and wettability of Si-DLC coatings, Mater. Res. Express 5 (2018), 036411.
[54] D. Schondelmaier, S. Cramm, R. Klingeler, J. Morenzin, C. Zilkens, W. Eberhardt, Orientation and self-assembly of hydrophobic fluoroalkylsilanes, Langmuir 18 (2002) 6242–6245.
[55] Z. Pan, H. Shahsavan, W. Zhang, F.K. Yang, B. Zhao, Superhydro-oleophobic bio-inspired polydimethylsiloxane micropillared surface via FDTS coating/blending approaches, Appl. Surf. Sci. 324 (2015) 612–620.
[56] M. Psarski, G. Celichowski, E. Bystrzycka, D. Pawlak, J. Grobelny, M. Cichomski, Vapor phase deposition of fluoroalkyl trichlorosilanes on silicon and glass: influence of deposition conditions and chain length on wettability and adhesion forces, Mater. Chem. Phys. 204 (2018) 305–314.
[57] H.Y. Erbil, Calculation of spreading pressure of water on cellulosic films from contact angle data, Turk. J. Chem. 21 (1997) 332–345.
[58] V. Kumar, J.R. Errington, Impact of Small-Scale Geometric Roughness on Wetting Behavior, Langmuir, 2013.
[59] A. Rana, A. Patra, M. Annamalai, A. Srivastava, S. Ghosh, K. Stoerzinger, Y.-L. Lee, S. Prakash, R.Y. Jueyuan, P.S. Goohpattader, N. Satyanarayana, K. Gopinadhan, M. M. Dykas, K. Poddar, S. Saha, T. Sarkar, B. Kumar, C.S. Bhatia, L. Giordano, Y. Shao-Horn, T. Venkatesan, Correlation of nanoscale behaviour of forces and macroscale surface wettability, Nanoscale 8 (2016) 15597–15603.
[60] M. Bartošík, L. Kormoš, L. Flajšman, R. Kalousek, J. Mach, Z. Lišková, D. Nezval, V. Švarc, T. Šamořil, T. Šikola, Nanometer-sized water bridge and pull-off force in AFM at different relative humidities: reproducibility measurement and model based on surface tension change, J. Phys. Chem. B 121 (2017) 610–619.
[61] M. Chyasnavichyus, S.L. Young, V.V. Tsukruk, Probing of polymer surfaces in the viscoelastic regime, Langmuir 30 (2014) 10566–10582.
[62] B. Bhushan, H. Liu, Nanotribological properties and mechanisms of alkylthiol and biphenyl thiol self-assembled monolayers studied by AFM, Phys. Rev. B 63 (2001) 245412.
[63] Z. Lu, A. Chernatynskiy, M.J. Noordhoek, S.B. Sinnott, S.R. Phillpot, Nanoindentation of ZrO2 and ZrO2/Zr systems by molecular dynamics simulation, J. Nucl. Mater. 486 (2017) 250–266.
[64] J.J.R. Rovira, E.J. Piqué, M.J. Anglada Gomila, Nanoindentation of advanced ceramics: applications to ZrO_2 materials, in: A. Tiwari, S. Natarajan (Eds.), Applied Nanoindentation in Advanced Materials, John Wiley & Sons Ltd, Oxford, UK, 2017, pp. 459–480.
[65] B. Bhushan, T. Kasai, G. Kulik, L. Barbieri, P. Hoffmann, AFM study of perfluoroalkylsilane and alkylsilane self-assembled monolayers for anti-stiction in MEMS/NEMS, Ultramicroscopy 105 (2005) 176–188.
[66] B. Bhushan, M. Cichomski, E. Hoque, A. DeRose, P. Hoffmann, J. Mathieu, Nanotribological characterization of perfluoroalkylphosphonate self-assembled monolayers deposited on aluminum-coated silicon substrates, Microsyst. Technol. 12 (2006) 588–596.
[67] Takeshi Matsuura, M.S. Khayet, Membrane Distillation: Principles and Applications, Elsevier, 2011.
[68] A. Alkhudhiri, N. Darwish, N. Hilal, Produced water treatment: application of air gap membrane distillation, Desalin. Water Treat. 309 (2013) 46–51.
[69] K.W. Lawson, D.R. Lloyd, Membrane distillation. II. Direct contact MD, J. Membr. Sci. 120 (1996) 123–133.
[70] J. Kujawa, W. Kujawski, Driving force and activation energy in air-gap membrane distillation process 69 (2015) 1438–1444.
[71] C.M. Guijt, G.W. Meindersma, T. Reith, A.B.d. Haan, Air gap membrane distillation: 2. Model validation and hollow fibre module performance analysis, Separ. Purif. Technol. 43 (2005) 245–255.
[72] A.M. Alklaibi, N. Lior, Transport analysis of air-gap membrane distillation, J. Membr. Sci. 255 (2005) 239–253.
[73] J. Straub, NBS/NRC steam tables. Von L. Haar, J. S. Gallagher und G. S. Kell. Hemisphere Publishing Corp., Washington–New York–London 1984. 1. Aufl., XII, 320 S., geb., $ 34.50, Chem. Ing. Tech. 57 (1985), 812-812.
[74] M. Tomaszewska, Membrane distillation - examples of applications in technology and environmental protection, Pol. J. Environ. Stud. 9 (2000) 27–36.
[75] C. Leger, H.D.L. Lira, R. Paterson, Preparation and properties of surface modified ceramic membranes. Part III. Gas permeation of 5 nm alumina membranes modified by trichloro-octadecylsilane, J. Membr. Sci. 120 (1996) 187–195.
[76] Y. Dong, L. Ma, C.Y. Tang, F. Yang, X. Quan, D. Jassby, M.J. Zaworotko, M. D. Guiver, Stable superhydrophobic ceramic-based carbon nanotube composite desalination membranes, Nano Lett. 18 (2018) 5514–5521.
[77] S. Tao, Y.-D. Xu, J.-Q. Gu, H. Abadikhah, J.-W. Wang, X. Xu, Preparation of high-efficiency ceramic planar membrane and its application for water desalination, J. Adv. Ceram. 7 (2018) 117–123.
[78] M.-Y. Yang, J.-W. Wang, L. Li, B.-B. Dong, X. Xin, S. Agathopoulos, Fabrication of low thermal conductivity yttrium silicate ceramic flat membrane for membrane distillation, J. Eur. Ceram. Soc. 39 (2–3) (2019) 442–448.
[79] J. Kujawa, S. Cerneaux, W. Kujawski, K. Knozowska, Hydrophobic ceramic membranes for water desalination, Appl. Sci. 7 (2017) 402.
[80] Y. Liao, R. Wang, M. Tian, C. Qiu, A.G. Fane, Fabrication of polyvinylidene fluoride (PVDF) nanofiber membranes by electro-spinning for direct contact membrane distillation, J. Membr. Sci. 425–426 (2013) 30–39.